Corona Discharges in Asymmetric Electrode Configurations

Miloud Kachi[1] and Lucien Dascalescu[2*]

[1] Electrical Engineering Laboratory, 8 May 1945 University, Guelma, 24000, Algeria

[2] PPRIME Institute, UPR 3346, CNRS University of Poitiers – ENSMA,
IUT d'Angoulême4, Av. de Varsovie, 16021 Angoulême, France
* E-mail: lucian.dascalescu@univ-poitiers.fr

Abstract— The dual corona electrode, consisting in an ionizing wire in parallel with a metallic cylindrical support, at same high voltage supply, has been extensively studied in relation with various electrostatic applications. In practical situations, the dual corona electrode may be installed in the proximity of metallic objects that will affect the electric field repartition and, hence, the development of the discharge. The aim of the present work is to analyze the operating conditions of such electrodes in the presence of metallic rods or plates connected at fixed or floating potential. The paper reports the results of current-voltage characteristics and current density repartition measurements for various configurations. The proximity of metallic objects leads to the increase of inception voltage and shifts the I-V characteristics to higher voltages. The objects at floating potential may reduce discharge current to very low values, while those energized at the same voltage as the ionizing wire may simply anneal the discharge.

INTRODUCTION

Various corona electrode arrangements have been developed and extensively studied in relation with such electrostatic applications as separation of granular materials, charging of electret air filters, or neutralization of charged insulating materials [1-9]. The efficiency of corona charging or neutralization processes depends on a multitude of factors, including the level, polarity or frequency of the high-voltage, as well as on the geometry of the electrode system [10-15].

Many electrode arrangements, using needles, pins or wires as corona emitting elements, are commonly employed in industrial applications [16, 17]. In such configurations, the electric field distribution and hence the corona discharge are symmetrical with respect to the electrode axis. In pin-plane or wire-plane electrode system, the current density distribution can be described by the empirical Warburg law [18]. Other symmetrical configurations have also been characterized in relation with various industry applications [19-21]. Recently, the modification of corona electrode by connecting a metallic cylinder in parallel with the energized wire was suggested as a solution to enhance the charge process of non-woven filter media [22, 23].
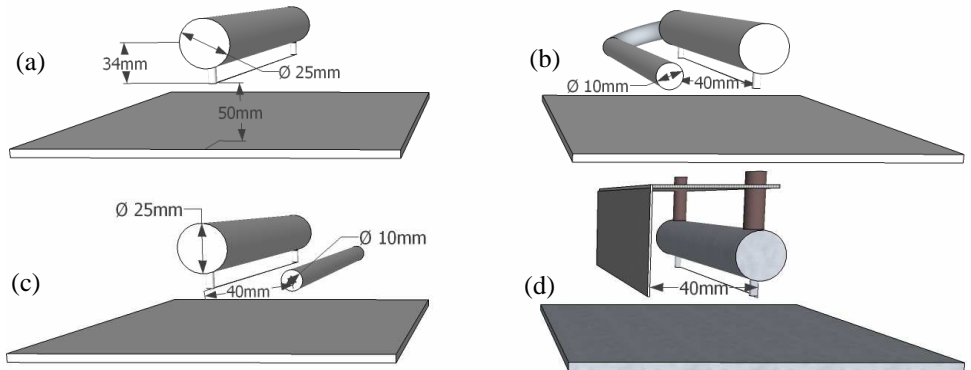
Fig. 1. "Standard" wire-type symmetric electrode arrangement (a) and asymmetric electrode arrangements, with cylindrical rod energized at the same voltage (b), with floating cylindrical rod (c) and floating plate (d).

In practical situations, the corona electrode may be installed in the close vicinity of metallic objects, such as metallic rods or plates connected at fixed or floating potential. This will modify the symmetry of the electric field repartition and, hence, the characteristics of the corona discharge. The objective is to quantify the effect of asymmetry on the current-voltage characteristics of the electrode system and on the repartition of current density at the surface of the non-ionizing (collecting) electrode

EXPERIMENTAL PROCEDURE

A. Electrode arrangements

The "standard" wire-type dual electrode consisted in a tungsten wire (0.2 mm in diameter) attached to a metallic cylinder (25 mm in diameter) and distanced at 34 mm from its axis (Fig. 1, a). The wire was located at 50 mm above the grounded electrode (aluminum plate, dimensions: 120 mm x 90 mm) and connected to an adjustable DC high voltage supply (positive polarity, 100 kV, 3 mA, Model SL 300, Spellman Inc.).

Two asymmetrical electrode arrangements were obtained by attaching a copper cylindrical rod (diameter: 10 mm) to the dual electrode. The rod, the axis of which was located at 40 mm from the wire, was either energized at the same voltage as the "standard" symmetric electrode (Fig. 1, b), or left at a floating potential (Fig. 1, c). For the third asymmetrical electrode, the rod was replaced by a profiled aluminum plate, at floating potential (Fig. 1, d).

B. Current density repartition measurements

The repartition of corona current was measured using a custom-designed printed circuit board (PCB) as collecting electrode (Fig. 2). Three voltage levels were considered, at both positive and negative polarity: 18 kV, 21 kV, and 24 kV. The current probe consisted in a rectangular sector (19 mm x 14 mm), insulated from the rest of the conductive plate, and connected to an electrometer (Keitheley Instruments, model 6514).
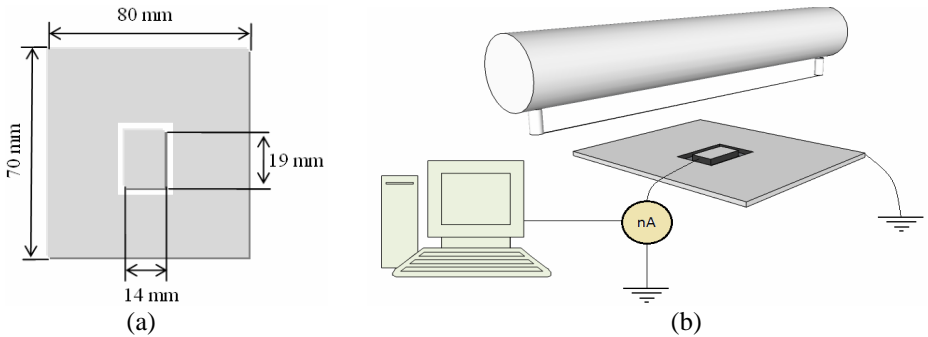
Fig. 2. Measurement of the corona current: (a) current probe and (b) measurement system for current distribution.

The PCB was mounted on a conveyer belt, so that the probe could modify its position with respect to the corona electrode system (Fig. 3). The measured current values were continuously recorded via a virtual instrument developed in LabView environment. Current density was then obtained by dividing the measured current by the surface of the probe.

C. Current - voltage characteristic measurements

The current - voltage characteristic was measured for the symmetric dual electrode in Fig. 1, a, and for the asymmetrical electrode arrangement in Fig. 1, c. The electrometer that was used for the measurement of the discharge current was placed between the collecting electrode and the ground. The high-voltage was read on the front panel of the DC power supply.

D. Surface potential measurements and neutralization efficiency evaluation

The experimental set up is given in Fig. 3. The granules of virgin polyethylene employed in the present study were quasi-spherical in shape and had a typical size of 3 mm. They were deposited as a mono-layer on a rectangular area of 7.5 cm x 8 cm on the surface of grounded plate electrode. The mass of such sample was 11 g.

The samples were first charged for 10 s from a wire-type "dual" corona electrode, using the triode-type electrode arrangement. A metallic grid was placed between the energized wire and the ground in order to control the corona charging process, as explained in a previous paper [7, 14]. The metallic grid consists of rhombic form loops (the distances between two adjacent nodes of the grid were respectively 6.4 mm and 4 mm. During the charging process the sample was placed, in fixed position, so that the centre of the granular layer was in the plane of symmetry of the electrode system.

As soon as the charge process was over, the belt conveyor moved the sample at constant speed (3 cm/s) beneath the probe (model 3450, Trek Inc.) of an electrostatic voltmeter (model 341B, Trek Inc.) to measure the repartition of the electric potential at the surface of the granular layer. The voltmeter was connected to a custom-designed data acquisition system, as described in [22].
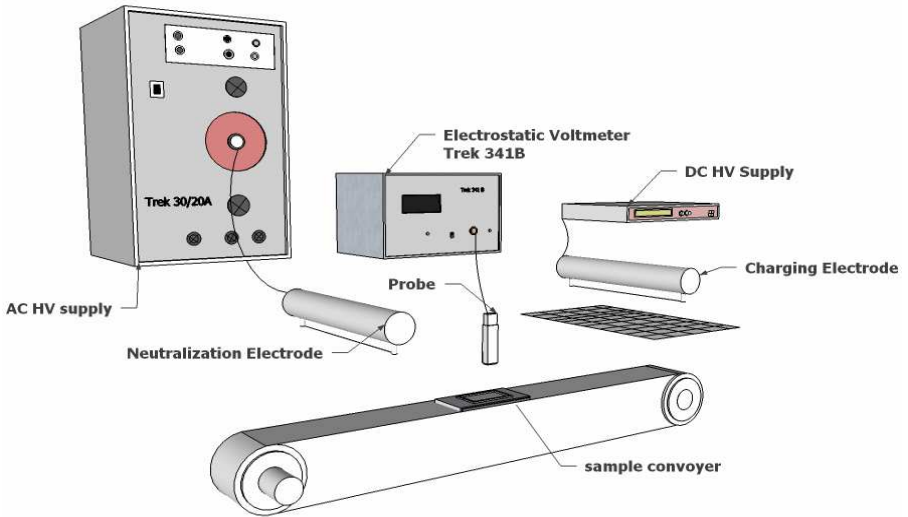
Fig. 3. Experimental setup

After that, the belt conveyor moved the sample beneath the neutralization electrode, at the same constant voltage (3 cm/s). In this way, the charged granular layer was exposed to the AC corona discharge generated by each of the four electrode arrangements in Fig. 1. In all cases, the wire electrode was situated at 5 cm above the charged sample and the sinusoidal neutralizing voltage had a peak value of 18 kV.

Finally, the efficiency of the neutralization was evaluated by measuring again the repartition of the potential due to the residual charge at the surface of the granular layer, using the electrostatic voltmeter probe, as described above. The surface potential measurements allow the quantification of the efficiency of neutralization process by comparing potential prior and after exposure to the corona discharge. The neutralization rate may be calculated as the ratio of maximum recorded potentials before and after neutralization [9, 15]:

$$N(\%) = \left(1 - \frac{V_{after}}{V_{before}}\right)100$$

RESULTS AND DISCUSSION

A. Current density repartition measurements

The repartition of discharge current density in the case of the symmetric wire-type dual electrode for two voltage level 18 kV and 21 kV, at positive and negative polarity, is displayed in Fig. 4. As expected, at same voltage level, the negative current has a higher absolute value than the positive one.

The current density repartition along the discharge zone for two asymmetric electrode configurations (floating plate and floating cylinder) are represented in Fig. 5.
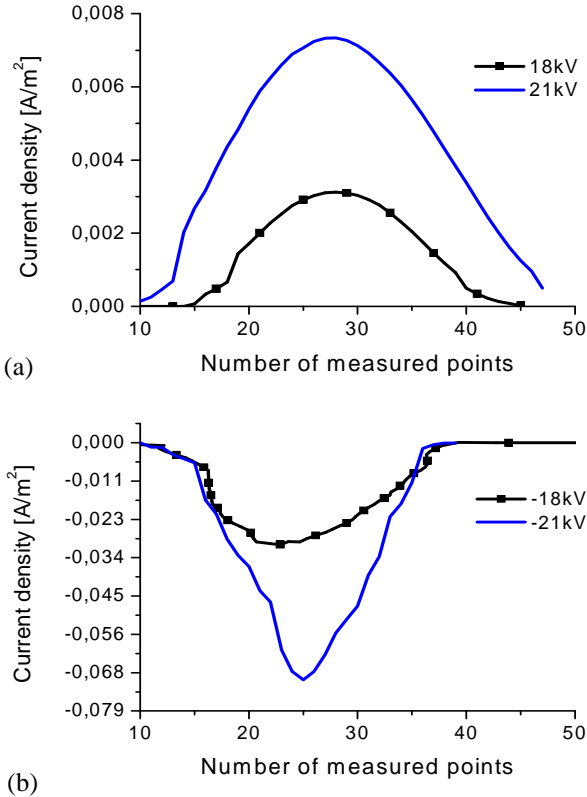
(a)

(b)

Fig. 4. Current density repartition for the symmetric wire-type dual electrode, at positive (a) and negative (b) voltage.

When the electrodes were energized at 18 kV, positive polarity, the current could be measured only in the case of the floating plate positive voltage experiments (Fig. 5, a); its value was lower than that measured for the symmetric electrode arrangement. The current recorded at this voltage in all the other cases of asymmetric electrode arrangements (not represented) was less than 1 nA.

At negative polarity, the voltage was increased to 21 and 24 kV to get more important current densities, and only the floating cylinder case is presented in the Fig. 5, b. At 21 kV, the maximum current density value obtained with the asymmetric electrode arrangement is not higher than 3 mA/m², while it exceeds 7 mA/m² for the same voltage in the case of symmetric electrode. This confirms that corona discharge process is significantly modified by the presence of metallic items near the electrode. This confirms that corona discharge process is significantly modified by the presence of metallic items near the electrode. However, for the fixed 5 cm inter-electrode distance considered in this study, the specific geometry of the electrode arrangements, and the relatively low resolution of the current probe, the asymmetry does not significantly affect the aspect of the current density repartition.
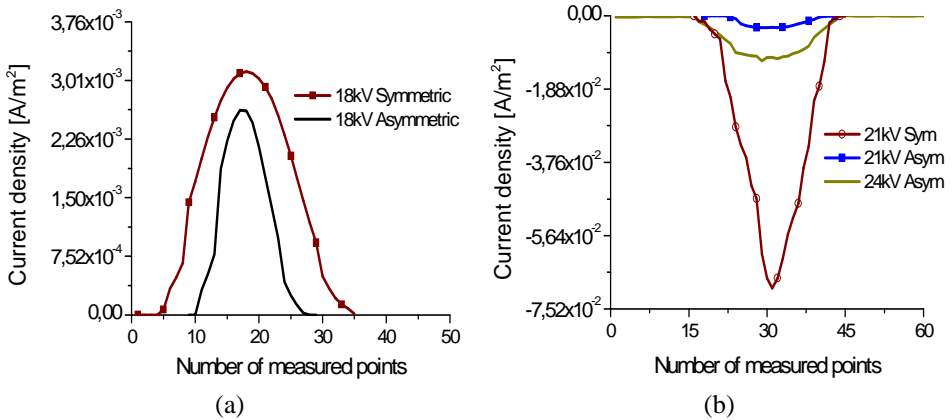
Fig. 5. Current density repartition for asymmetric electrode arrangements: (a) floating plate, at positive voltage; (b) floating cylinder, at negative voltage. The curves obtained for the symmetric wire-type dual electrode are also represented, to facilitate the comparison.

B. *Current-voltage characteristics*

Fig. 6 displays the I-V characteristics obtained for symmetric and asymmetric (floating cylinder) electrode arrangements. Obviously, asymmetry causes the shift of the I-V characteristic to higher voltages. Indeed, the inception voltage becomes higher for asymmetric electrode arrangements, as a direct consequence of field modification near the discharge wire.
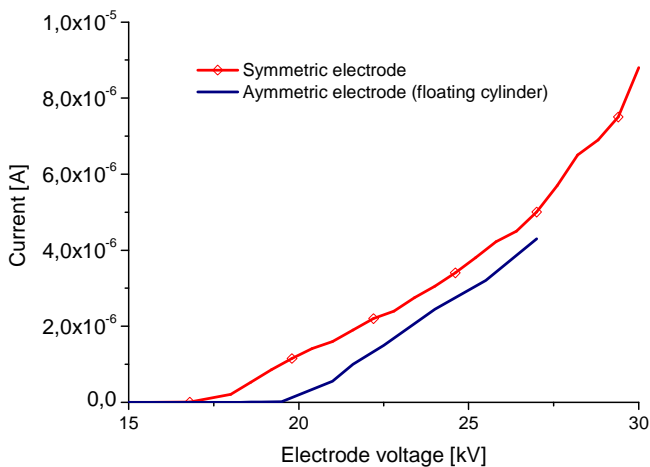

Fig. 6. Current-voltage characteristics of the symmetric wire-type dual electrode and the asymmetric floating rod electrode arrangement.

C. Surface potential repartition and neutralization efficiency

Fig. 7 shows typical surface potential repartitions at the surface of granular layers before and after exposure to the neutralizing discharge, for the four electrode arrangements in Fig. 1.
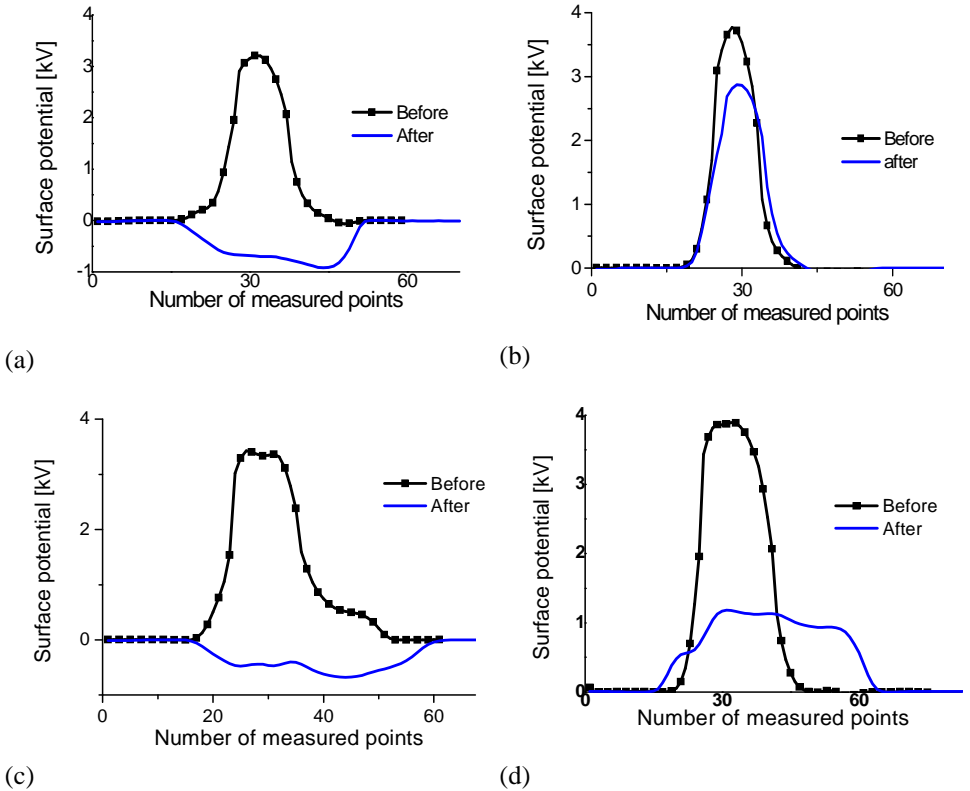

(a)

(b)

(c)

(d)

Fig. 7. Surface potential distribution prior and after neutralization for the considered electrode configurations: (a) symmetric wire-type dual electrode; (b) asymmetric electrode arrangement, with rod at same potential with the wire; (c) asymmetric electrode arrangement, with rod at floating voltage; (d) asymmetric electrode arrangement with plate at floating potential. (AC neutralizing voltage: 18 kV, peak value; inter-electrode distance: 5cm).

The neutralization efficiency is dependent on electrode configuration. Based on the data recorded in three repetitions, the average neutralization rate obtained with the symmetric wire-type dual electrode is 71.3% (Fig. 7, a). The asymmetric electrode arrangement with rod connected to the same potential (Fig. 7, b) engenders a feeble neutralization rate of 23.6%. This points out that the discharge process is strongly weakened by the presence of the energized rod in the proximity of the discharge wire, and the charged granular layer cannot be properly neutralized. For asymmetric electrode with floating items, either rod or plate (Fig. 7, c, d), the neutralization rate (80% and 69.7% respectively for floating rod and floating plate) is similar to that obtained with the symmetrical dual electrode.

CONCLUSIONS

The current-voltage characteristics point out that the asymmetry of the corona discharge electrode arrangements is accompanied by the increase of the inception voltage. The corona current measured at any given voltage is lower than for the symmetrical wire-type dual electrode.

Under the conditions of the experiments described in this paper, the current density at the surface of the collecting electrode is drastically reduced by the presence of objects at the same voltage as the corona wire or at floating potential, but its repartition has an aspect that is not significantly altered by the asymmetry of the electric field.

As a consequence of the decrease of the discharge current, a neutralizer provided with a symmetrical electrode intended to operate at a given voltage can be found totally ineffective as a result of asymmetry caused by the proximity of a metallic object.

REFERENCES

[1]   A.D. Moore (Ed), *Electrostatics and Its Applications*. New York: Wiley, 1973.
[2]   J.S Chang, A.J. Kelly, and J.M. Crowley (Eds), *Handbook of Electrostatic Processes*. New York: Dekker, 1995.
[3]   Y. Higashiyama and K. Asano, "Recent progress in electrostatic separation technology," *Part. Sci. & Technol.*, Vol. 16, pp. 77-90, 1998.
[4]   A. Bendaoud, L. Dascalescu, M. Blajan, A. Samuila, A. Stochita, and P Notingher, "Corona charging of granular layers of insulating particles at the surface of a grounded electrode." *J. Electrostat.*, Vol. 63, pp. 643-647, 2005.
[5]   A. Samuila, M. Blajan, R. Beleca, M. Huzau, R. Morar, L. Dascalescu, and A. Iuga, "Modeling of wire corona electrode operation in electrostatic separation at small and large gaps." *J. Electrostat.*, Vol. 63, pp.955-960, 2005.
[6]   L.M. Dumitran, O. Blejan, P.V. Notingher, A. Samuila, and L. Dascalescu, "Particle charging in combined corona-electrostatic fields," *IEEE Trans. Ind. Appl.*, Vol. 44, pp. 1385-1390, 2008.
[7]   B. Tabti, R. Mekideche, M. Plopeanu, L.M. Dumitran, L. Herous, L. Dascalescu, "Corona charging and charge decay characteristics of non-woven filter media," *IEEE Trans. Ind. Appl.*, Vol. 46, pp. 634-640. 2010.
[8]   A. Antoniu, A. Smaili, I. Vacar, M. Plopeanu, and L. Dascalescu, "Sinusoidal and triangular high-voltage neutralizers for accelerated discharge of non-woven fibrous dielectrics," *IEEE Trans. Ind. Appl.*, Vol. 48, pp. 857-863, 2012.
[9]   M. Kachi, L. Dascalescu**,** L. Herous, and M. Nemamcha, "Experimental study of charge neutralization at the surface of granular layers of insulating material," *IEEE Trans. Ind. Appl.*, Vol. 49, pp. 691-698, 2013.
[10] C. G. Noll, "Balanced static elimination in variable ion mobility environnements," *J Electrostat,* Vol. 49, pp. 169 - 194, 2000.
[11] J. S. Chang and A. A. Berezin, "Neutralization of static surface charges by a flow stabilized corona discharge ionizer in a nitrogen environnement," *J. Electrostat.*, vol. 51 - 52, pp. 64 - 70, 2001.
[12] A. Ohsawa, "Modelling of charge neutralization by ionizer," *J. Electrostat.*, vol. 63, pp. 767- 773, 2005.
[13] K. Asanoa, Y. Fukadab, and T. Yasukawa, "Measurement of AC ion current from a corona ionizer using a Faraday cage," *J. Electrostat.*, vol. 66, pp. 275 – 282, 2008.
[14] B. Tabti, L. Dascalescu**,** C.M. Plopeanu, A. Antoniu, and R. Mekideche, "Factors that influence the corona charging of fibrous dielectric materials." *J. Electrostat.*, vol. 69, pp.193-197, 2009.

[15] M. Kachi, M. Nemamcha, L. Herous, and L. Dascalescu, "Neutralization of charged insulating granular materials using AC corona discharge," *J. Electrostat.,* Vol. 69, pp. 296 - 301, 2011.

[16] L. Dascalescu, A. Iuga, R. Morar, V. Neamtu, I. Suarasan, A. Samuila, and D. Rafiroiu, "Corona and electrostatic electrodes for high-tension separators." *J. Electrostat.,* Vol. 29. pp. 211-225, 1993.

[17] A. Bendaoud, A. Tilmatine, K. Medles, M. Blajan, M. Rahli, and L. Dascalescu, "Caractérisation expérimentale des électrodes couronne de type dual," *J. Electrostat.,* Vol. 64. pp. 431-436, 2006.

[18] M. Goldman, A. Goldman and R. S. Sigmond, "The corona discharge, its properties and specific uses", *Pure & AppL. Chem.*, Vol. 57, pp. 1353 - 1362, 1985.

[19] G. Mischkulnig and P. Bento, "Enhanced corona discharge using innovative rigid discharge electrodes (RDE)," 9th International Conference on Electrostatic Precipitation, South Africa, 2004.

[20] P. Intra and N. Tippayawong, "Effect of needle cone angle and air flow rate on electrostatic discharge characteristics of corona-needle ionizer," *J. Electrostat.,* Vol. 68, pp.254-260, 2010.

[21] K. Seok Choi, T. Mogami, T. Suzuki, S. Kim, and M. Yamaguma, "Charge reduction on polypropylene granules and suppression of incendiary electrostatic discharge by using a novel AC electrostatic ionizer," *Journal of Loss Prevention in the Process Industries*. Vol. 26, pp. 255-260, 2013.

[22] M.C. Plopeanu, L. Dascalescu, B. Yahiaoui, A. Antoniu, M. Hulea, and P. Notingher, "Repartition of electric potential at the surface of non-woven fabrics for air-filtration," *IEEE Trans. Ind. Appl.*, Vol. 48, pp. 851-856.

[23] M.C. Plopeanu, L. Dascalescu, B. Neagoe, A. Bendaoud, and P. Notingher "Charactrerization of two electrode systems for corona charging of non-woven filter media," *J. Electrostat.,* Vol. 71, pp. 517-523. 2013.